

Provided for non-commercial research and education use.
Not for reproduction, distribution or commercial use.



This article appeared in a journal published by Elsevier. The attached copy is furnished to the author for internal non-commercial research and education use, including for instruction at the authors institution and sharing with colleagues.

Other uses, including reproduction and distribution, or selling or licensing copies, or posting to personal, institutional or third party websites are prohibited.

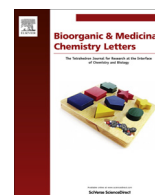
In most cases authors are permitted to post their version of the article (e.g. in Word or Tex form) to their personal website or institutional repository. Authors requiring further information regarding Elsevier's archiving and manuscript policies are encouraged to visit:

<http://www.elsevier.com/authorsrights>



Contents lists available at ScienceDirect

Bioorganic & Medicinal Chemistry Letters

journal homepage: www.elsevier.com/locate/bmcl

Discovery of ZAP70 inhibitors by high-throughput docking into a conformation of its kinase domain generated by molecular dynamics



Hongtao Zhao, Amedeo Caflisch*

Department of Biochemistry, University of Zurich, Winterthurerstrasse 190, CH-8057 Zurich, Switzerland

ARTICLE INFO

Article history:

Received 10 July 2013

Revised 30 July 2013

Accepted 1 August 2013

Available online 11 August 2013

Keywords:

Tyrosine kinase

High-throughput docking

Molecular dynamics

Autoimmune disease

ABSTRACT

Very few selective inhibitors of the zeta-chain associated protein kinase 70 kDa (ZAP70) have been reported despite its importance in autoimmune diseases. Here, to induce a fit of the so-called gatekeeper residue (Met414) and hydrophobic pocket next to it, a potent Janus kinase 2 (JAK2) inhibitor was first docked into the ATP binding site of ZAP70 by structural alignment of the kinase domains. The resulting model of the complex between ZAP70 and the JAK2 inhibitor was then relaxed by an explicit solvent molecular dynamics simulation with restraints on the backbone atoms. High-throughput docking into the induced-fit conformation of ZAP70 generated by molecular dynamics has revealed 10 low-micromolar inhibitors which correspond to six distinct chemotypes. One of these ZAP70 inhibitors has an IC_{50} of 110 nM for JAK2.

© 2013 Elsevier Ltd. All rights reserved.

Zeta-associated protein 70 kDa (ZAP70), a member of the Syk family and non-receptor protein tyrosine kinases mainly expressed on T cells and natural killer cells, plays a crucial role in immune response and is implicated in inflammatory and autoimmune diseases.^{1,2} Thus, ZAP70 is an attractive therapeutic target for various allergic and autoimmune disorders as well as immunosuppressive therapy following organ transplantation. Although four series of small-molecule ZAP70 inhibitors have been reported (Fig. 1),^{3–7} a cell-permeable and highly specific ZAP70 inhibitor has not been identified as of today.² Most ATP-competitive kinase inhibitors promiscuously inhibit multiple kinases. On the other hand, a recent comprehensive selectivity profiling of 178 commercially available small molecule inhibitors on a panel of 300 recombinant protein kinases revealed that ZAP70 is one of the least druggable by chemical inhibition,⁸ which was further confirmed by another profiling of 72 inhibitors on 442 kinases.⁹

Previously we have discovered three novel classes of tyrosine kinase inhibitors,^{10–12} which bind into the ATP site occupying the hydrophobic back pocket (PDB codes 4G2F¹² and 4GK2¹³). Optimization of the moieties in the back pocket leads to potent and selective tyrosine kinase inhibitors^{12,13} starting from initial hits that are low micromolar binders (Fig. 2).^{10,12} Targeting the back pocket is a common strategy to gain both potency and selectivity in kinase drug design.¹⁴

The access of the back pocket is modulated by the so-called gatekeeper residue. ZAP70 has a bulky gatekeeper residue (Met414) which blocks the entry of the back pocket and thus renders it inaccessible to small molecules as shown in the crystal structures of the ZAP70/staurosporine and ZAP70/ATP-derived inhibitor (PDB code 1U59⁴ and 2OZO,¹⁵ respectively). However, analysis of complex structures of kinases with a bulky Met gatekeeper residue in the Protein Data Bank reveals that the back pocket of some kinases such as JAK2¹⁶ and JNK3¹⁷ still can be accessed by potent small-molecule inhibitors. Although belonging to a different subfamily and sharing low overall sequence identity of 35% with ZAP70, JAK2 (PDB code 3KCK¹⁶) shows a high geometric similarity in the ATP site with ZAP70 (PDB code 1U59⁴). Automatic placement of a sub-nanomolar JAK2 inhibitor¹⁶ (whose chemical structure is shown in Figure 3) into the ZAP70 ATP-binding site by structural alignment of the backbone C_{α} atoms of the two crystal structures reveals only minor van der Waals clashes. Following a protocol developed recently in our group,¹⁸ a 2-ns explicit solvent molecular dynamics simulation of ZAP70 complexed with the JAK2 inhibitor was carried out to induce a fit of the gatekeeper residue Met414 and the back pocket side chains, so that the slight clashes can be removed by minor side chain displacements to allow exploration of the back pocket. Use of harmonic restraints on the C_{α} atoms of ZAP70 (force constant of $1 \text{ kcal mol}^{-1} \text{ \AA}^{-2}$) during the molecular dynamics run guarantees that the overall structure of the kinase domain is not perturbed by the presence of the inhibitor (Fig. S1). To select a single structure for high-throughput docking, the 500 snapshots saved during the second half (from 1 ns to

* Corresponding author. Tel.: +41 446355521; fax: +41 446356862.

E-mail address: caflisch@bioc.uzh.ch (A. Caflisch).

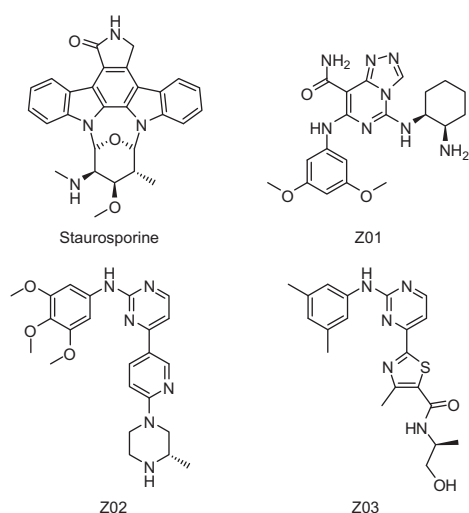


Figure 1. Four series of previously reported nanomolar inhibitors of ZAP70.^{3–7}

2 ns) of the molecular dynamics trajectory were first filtered by three hydrogen bonds formed between the JAK2 inhibitor and ZAP70 (two with the hinge region and one with the backbone NH of Phe480 in the back pocket) using a cutoff of 2.4 Å between the donor hydrogen and acceptor atoms. The JAK2 inhibitor was then re-docked into each of the 19 snapshots that survived the filtering, and the one with the most favorable docking score¹¹ was selected for high-throughput docking. This snapshot is called molecular dynamics induced-fit structure in the following.

The high-throughput docking protocol is illustrated in Figure 3. The ZINC-all now library¹⁹ (version of 2011) was first filtered to generate a kinase focused library with the following physicochemical properties: (1) Molecular weight (Mw) smaller than 380 g/mol; (2) less than 8 rotatable bonds; (3) at least one hydrogen bond donor and two acceptors; (4) number of rings from 3 to 5 based on the observation of type I kinase inhibitors and size of the ATP binding site. Using these filters, the initial library of nearly 9 million compounds was reduced to a focused library of about 750,000 molecules. The focused library was then docked into the molecular dynamics induced-fit structure of ZAP70 by an in-house developed fast docking tool, which is based on a combination of simulated

annealing and genetic algorithm optimization of position, orientation, and rotatable bonds of the ligand (H. Zhao and A. Caflisch, manuscript in preparation). The docking poses were further minimized in the rigid protein by CHARMM^{20,21} with the CHARMM22 force field.²² The poses were then subject to three filters: van der Waals efficiency (i.e., intermolecular van der Waals energy divided by Mw) more favorable than -0.1 kcal/g,¹⁸ hydrogen bonding penalty¹¹ smaller than 2, and presence of at least two hydrogen bonds to the hinge, to gain computational efficiency by removing unrealistic poses before rescoring by a computationally expensive energy function. The 755,837 poses of the 280,021 compounds that survived these filters were ranked according to a previously reported scoring function,¹¹ which has been used to identify novel classes of kinase inhibitors with activity ranging from low micromolar to nanomolar.^{11,12,18} Finally, 30 compounds selected by visual inspection of the top ranking poses (seven of which were predicted to address the back-pocket) were purchased for bioassay.

The IC₅₀ (inhibitor concentration at which 50% of the enzymatic activity is observed) measurements on full-length ZAP70 were carried out at Reaction Biology Corp. with radioactive ATP at 1 μM concentration. Notably, eight compounds structurally different from the ZAP70 inhibitors reported in the literature (Figure 1) showed low-micromolar inhibitory activity against ZAP70, with the most active being 8 μM (Figure 4 and Table 1). The remaining 22 compounds are inactive at a test concentration of 20 μM and are shown in the Supplementary data (Figure S2). In addition, derivatives of compound 5 with Mw greater than 380 g/mol were retrieved by substructure search and docked. Compounds 6 and 7 based on the docking results were then selected for the enzymatic assay in which they also show low-micromolar activity for ZAP70 (Table 1). These 10 inhibitors of ZAP70 are predicted to form at least two hydrogen bonds with Ala417 of the hinge, a segment linking the N- and C-lobe of the kinase domain (Figs. 5 and 6). Compounds 2, 3, 9 and 10 form an additional hydrogen bond with the backbone carbonyl group of Glu415 of the hinge. Such hydrogen bonding pattern is a typical feature of hinge binders, mimicking ATP binding. Note in this context that only compound 10 shares part of its scaffold (anilino-pyrimidine) with one of the known inhibitors of ZAP70 (Z02, and to a less extent Z03 in Figure 1) while the other 9 inhibitors are novel.

It is difficult to correlate structural features and/or individual intermolecular interactions with activity because all of the 10 inhibitors have similar potency, that is, within the very small range

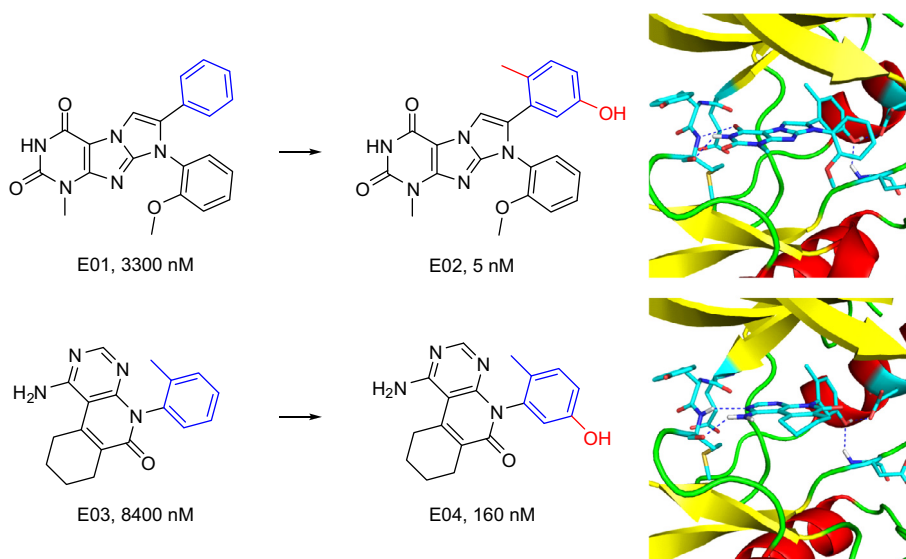


Figure 2. Hit to lead by optimization of the moieties (colored in blue) in the back pocket, and crystal structures of E02 (PDB code 4GK2) and E04 (PDB code 4G2F) bound to the kinase domain of EphA3.^{12,13} Dashed lines represent intermolecular hydrogen bonds. The hydroxyl group forms two buried hydrogen bonds with the DFG motif and the side chain of the catalytically important Glu.

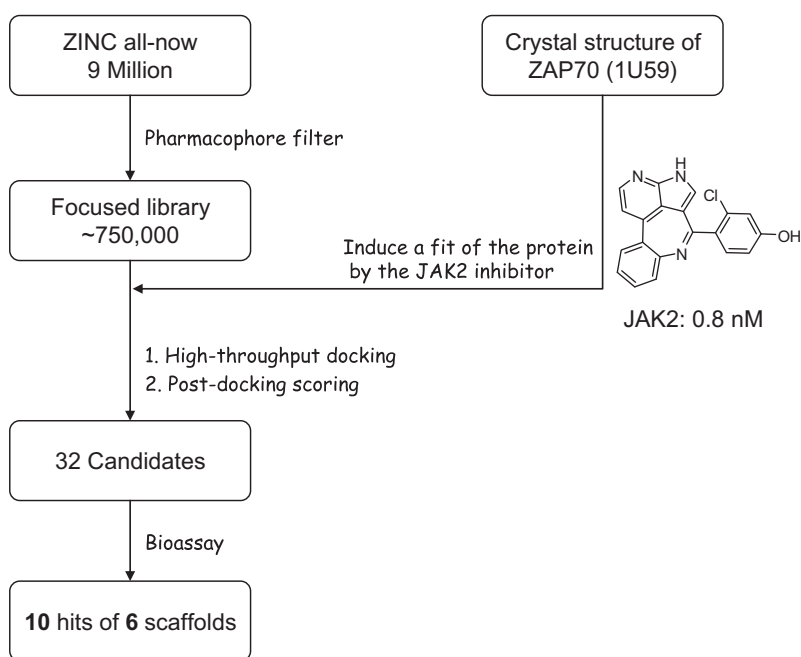


Figure 3. Flow chart of the high-throughput docking protocol.

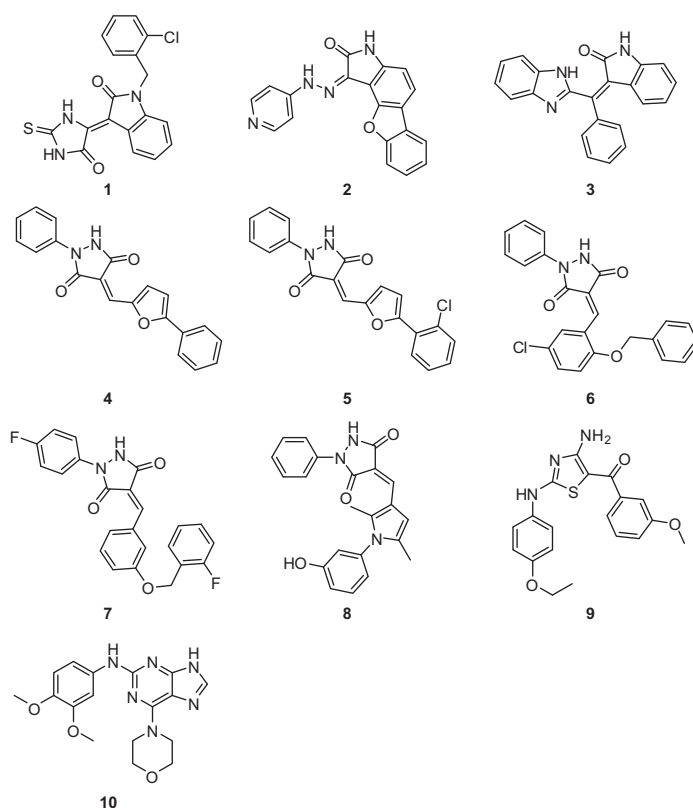


Figure 4. ZAP70 inhibitors identified by high-throughput docking into a conformation generated by molecular dynamics.

of 10–100 μM . Compounds **2** and **3** share a 2-indolinone fragment interacting with the hinge whereas the same fragment does not interact with the hinge in compound **1** (Fig. 5). Compounds **4–8** share a phenylpyrazolidine-3,5-dione fragment forming two hydrogen bonds with the hinge. It has to be noted that compounds **4–8** contain a potentially active Michael-system, which might pre-

vent from further developing them into more potent inhibitors without replacement of the core scaffold.²³ Compounds **1**, **2**, **9** and **10** do not reach deep into the hydrophobic back pocket (Fig. 5), and their binding mode can be reproduced by docking into the crystal structure of ZAP70 in the complex with staurosporine (1U59). In contrast, compounds **4–6** occupy the back pocket with

Table 1
Values of IC₅₀ in μM or %inhibition at 20 μM concentration of compound^a

Compound	ZAP70	SYK	JAK2
1	21	168	ND ^b
2	8	26	11
3	26	40	ND
4	(49%)	(17%)	ND
5	14	57	6
6	22	(16%)	15
7	(46%)	(16%)	(22%)
8	(43%)	(16%)	ND
9	29	>200	ND
10	62	12	0.11

^a These values were obtained by an enzymatic assay with radioactive ATP at 1 μM concentration carried out at Reaction Biology Corp using a 10-dose response protocol. Dose–response curves for compounds **2**, **5** and **10** are shown in Figure S2. Values of %inhibition are averages of two measurements and are shown in parentheses.

^b Not determined.

a phenyl ring (Fig. 6), and thus cannot be docked into the ZAP70/staurosporine structure because of steric clashes. Although compounds **5** and **6** have two different linkers, the head and tail moieties are essentially overlapped in the docked poses (Fig. 6, left bottom).

Syk family inhibitors typically inhibit spleen tyrosine kinase (Syk) and ZAP70, which are closely related.^{8,9,24} Interestingly, some compounds such as **1**, **2**, **5**, **6** and **9** are more potent against ZAP70 than Syk (Table 1). Given their relatively low Mw (below 380 Da because of the initial filter) they might serve as starting points for hit optimization into potent and selective ZAP70 inhibitors. In particular, modifications of compounds **5** and **6** are likely to improve their potency. Previously, we have shown that the addition of a hydroxyl group to the moiety in the back pocket can lead to an increase in binding affinity by a factor of more than 50 (Fig. 2).^{12,13} As shown in Figure 6 (right bottom), addition of a hydroxyl group to the phenyl ring in the back pocket is predicted to result in two additional hydrogen bonds with Phe480 of the DFG motif and the catalytically important Glu386. As a second possible modification of compounds **5** and **6**, the additional carboxyl group at the solvent accessible phenyl ring would form a salt bridge with the Lys424 side chain which is specific for ZAP70 and might thus improve both affinity and selectivity and result also in an increase in solubility.

Since JAK2 shares a high similarity in the ATP binding site with ZAP70, some of the ZAP70 inhibitors were also tested on JAK2.

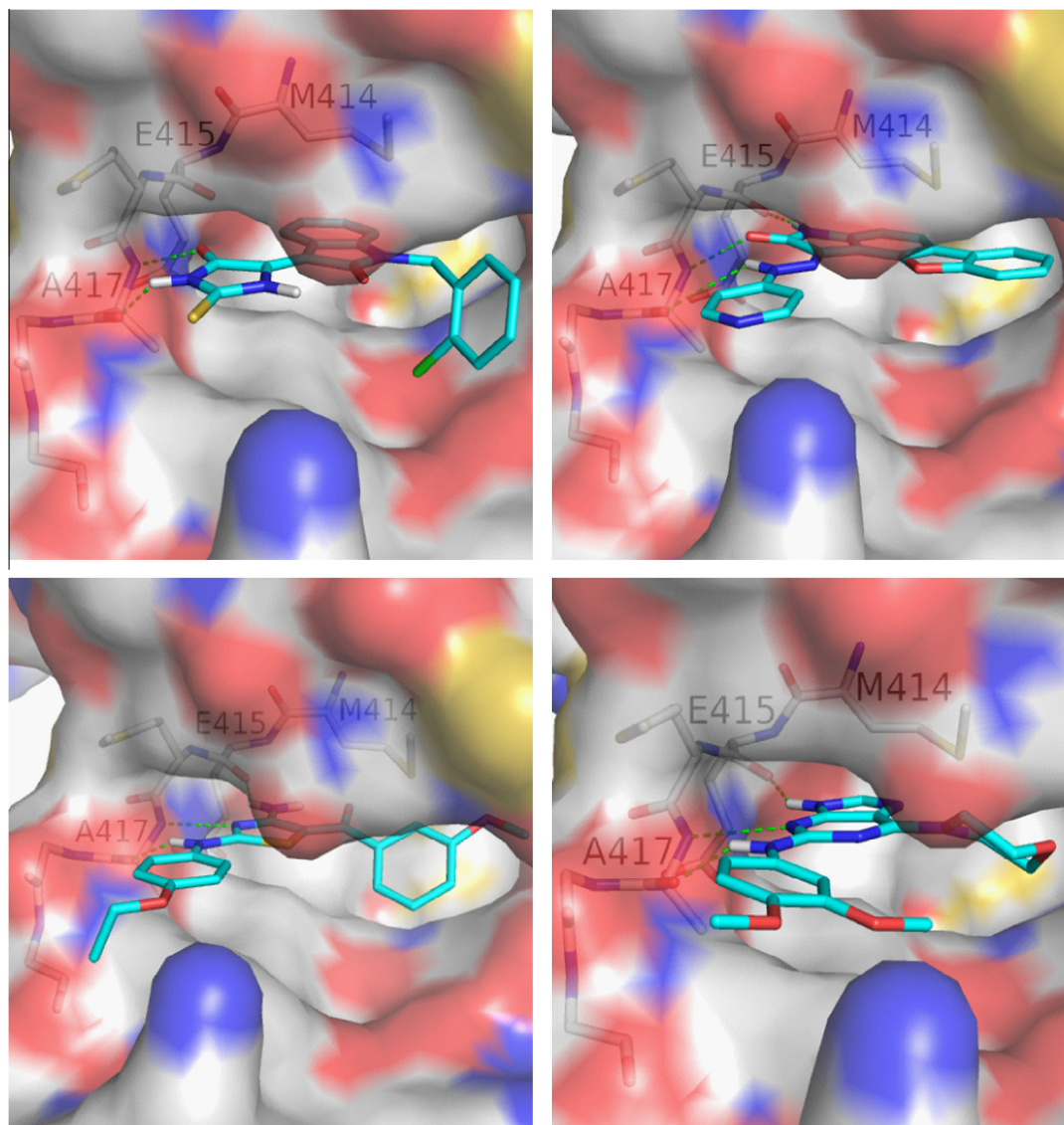


Figure 5. Predicted binding modes of compounds **1**, **2**, **9** and **10** in the molecular dynamics induced-fit structure of ZAP70. Dashed lines represent intermolecular hydrogen bonds.

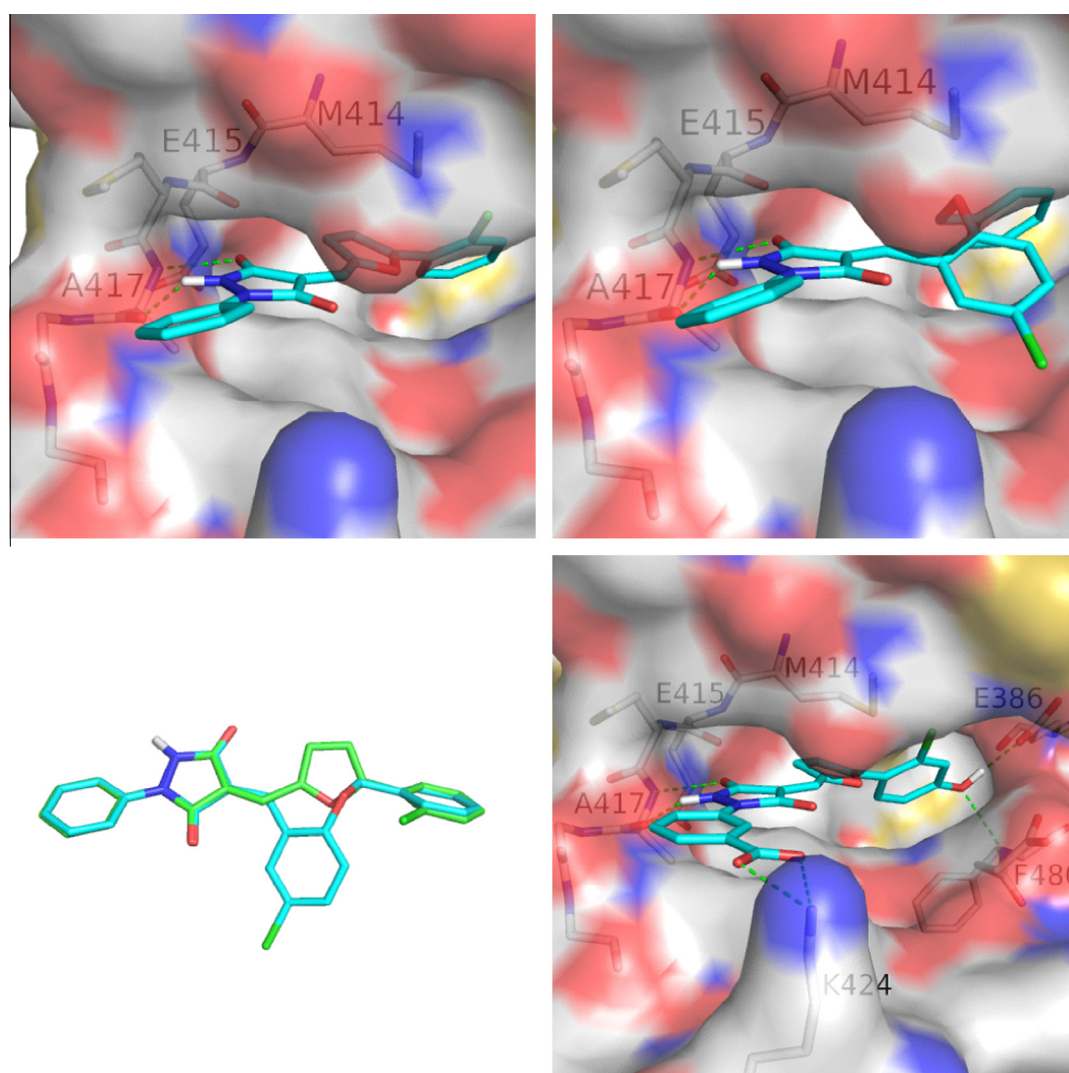


Figure 6. (Top) Predicted binding modes of compounds **5** and **6** in the molecular dynamics induced-fit structure of ZAP70. (Bottom left) Structural overlap of the docked poses of compounds **5** and **6**. (Bottom right) Suggested optimization of compound **5**. Dashed lines represent intermolecular hydrogen bonds. The additional hydroxyl group would form two buried hydrogen bonds with F480 and E386. The additional carboxyl group involved in a salt bridge with Lys424 is expected to improve selectivity and potency.

Compounds **2**, **5**, and **6** show similar low-micromolar activity on JAK2 and ZAP70 (Table 1). On the other hand, compound **10** has an IC_{50} of 110 nM for JAK2 which is almost three orders of magnitude more favorable than for ZAP70. This finding indicates that the screening panel of kinases should include kinases sensitive to chemical inhibition⁸ and with high similarity in the ATP-binding site to the primary target to discover off-target effects.

In summary, we have discovered six chemotypes of inhibitors of the ZAP70 tyrosine kinase by high-throughput docking into a conformation of its catalytic domain generated by molecular dynamics in the presence of a JAK2 inhibitor. The molecular dynamics simulation protocol used in this work to prepare the ZAP70 structure for docking, that is, to increase the aperture of (sub-pockets of) the binding site without significantly altering the protein backbone, is likely to be useful whenever the three-dimensional structure of the complex of a cognate enzyme and (potent) inhibitor is available.

Acknowledgments

We are grateful to Armin Widmer (Novartis Basel) for the continuous support with the program WITNOTP, which was used

for visual analysis. Calculations were performed on the Schroedinger cluster at the Informatikdienste of University of Zurich. This work was supported by the Swiss National Science Foundation.

Supplementary data

Supplementary data associated with this article can be found, in the online version, at <http://dx.doi.org/10.1016/j.bmcl.2013.08.009>.

References and notes

- Wang, H.; Kadlecak, T. A.; Au-Yeung, B. B.; Goodfellow, H. E.; Hsu, L. Y.; Freedman, T. S.; Weiss, A. *Cold Spring Harb. Perspect. Biol.* **2010**, *2*, a002279.
- Au-Yeung, B. B.; Levin, S. E.; Zhang, C.; Hsu, L. Y.; Cheng, D. A.; Killeen, N.; Shokat, K. M.; Weiss, A. *Nat. Immunol.* **2010**, *11*, 1085.
- Moffat, D.; Davis, P.; Hutchings, M.; Davis, J.; Berg, D.; Batchelor, M.; Johnson, J.; O'Connell, J.; Martin, R.; Crabbe, T.; Delgado, J.; Perry, M. *Bioorg. Med. Chem. Lett.* **1999**, *9*, 3351.
- Jin, L.; Pluskey, S.; Petrella, E. C.; Cantin, S. M.; Gorga, J. C.; Rynkiewicz, M. J.; Pandey, P.; Strickler, J. E.; Babine, R. E.; Weaver, D. T.; Seidl, K. J. *J. Biol. Chem.* **2004**, *279*, 42818.
- Hirabayashi, A.; Mukaiyama, H.; Kobayashi, H.; Shiohara, H.; Nakayama, S.; Ozawa, M.; Tsuji, E.; Miyazawa, K.; Misawa, K.; Ohnota, H.; Isaji, M. *Bioorg. Med. Chem.* **2008**, *16*, 9247.

6. Hirabayashi, A.; Mukaiyama, H.; Kobayashi, H.; Shiohara, H.; Nakayama, S.; Ozawa, M.; Miyazawa, K.; Misawa, K.; Ohnota, H.; Isaji, M. *Bioorg. Med. Chem.* **2009**, *17*, 284.
7. Farmer, L. J.; Bemis, G.; Britt, S. D.; Cochran, J.; Connors, M.; Harrington, E. M.; Hooek, T.; Markland, W.; Nanthakumar, S.; Taslimi, P.; Ter Haar, E.; Wang, J.; Zhaveri, D.; Salituro, F. G. *Bioorg. Med. Chem. Lett.* **2008**, *18*, 6231.
8. Anastasiadis, T.; Deacon, S. W.; Devarajan, K.; Ma, H.; Peterson, J. R. *Nat. Biotechnol.* **2011**, *29*, 1039.
9. Davis, M. I.; Hunt, J. P.; Herrgard, S.; Ciceri, P.; Wodicka, L. M.; Pallares, G.; Hocker, M.; Treiber, D. K.; Zarrinkar, P. P. *Nat. Biotechnol.* **2011**, *29*, 1046.
10. Kolb, P.; Kipouros, C. B.; Huang, D.; Caffisch, A. *Proteins* **2008**, *73*, 11.
11. Zhao, H.; Huang, D. *PLoS One* **2011**, *6*, e19923.
12. Zhao, H.; Dong, J.; Lafleur, K.; Nevado, C.; Caffisch, A. *ACS Med. Chem. Lett.* **2012**, *3*, 834.
13. Lafleur, K.; Huang, D.; Zhou, T.; Caffisch, A.; Nevado, C. *J. Med. Chem.* **2009**, *52*, 6433.
14. Zuccotto, F.; Ardini, E.; Casale, E.; Angiolini, M. *J. Med. Chem.* **2010**, *53*, 2681.
15. Deindl, S.; Kadlecsek, T. A.; Brdicka, T.; Cao, X.; Weiss, A.; Kuriyan, J. *Cell* **2007**, *129*, 735.
16. Wang, T.; Ledebner, M. W.; Duffy, J. P.; Salituro, F. G.; Pierce, A. C.; Zuccola, H. J.; Block, E.; Shlyakter, D.; Hogan, J. K.; Bennani, Y. L. *Bioorg. Med. Chem. Lett.* **2010**, *20*, 153.
17. Scapin, G.; Patel, S. B.; Lisnock, J.; Becker, J. W.; LoGrasso, P. V. *Chem. Biol.* **2003**, *10*, 705.
18. Zhao, H.; Huang, D.; Caffisch, A. *ChemMedChem* **2012**, *7*, 1983.
19. Irwin, J. J.; Shoichet, B. K. *J. Chem. Inf. Model.* **2005**, *45*, 177.
20. Brooks, B. R.; Bruccoleri, R. E.; Olafson, B. D.; States, D. J.; Swaminathan, S.; Karplus, M. *J. Comput. Chem.* **1983**, *4*, 187.
21. Brooks, B. R.; Brooks, C. L., 3rd; Mackerell, A. D., Jr.; Nilsson, L.; Petrella, R. J.; Roux, B.; Won, Y.; Archontis, G.; Bartels, C.; Boresch, S.; Caffisch, A.; Caves, L.; Cui, Q.; Dinner, A. R.; Feig, M.; Fischer, S.; Gao, J.; Hodoscek, M.; Im, W.; Kuczera, K.; Lazaridis, T.; Ma, J.; Ovchinnikov, V.; Paci, E.; Pastor, R. W.; Post, C. B.; Pu, J. Z.; Schaefer, M.; Tidor, B.; Venable, R. M.; Woodcock, H. L.; Wu, X.; Yang, W.; York, D. M.; Karplus, M. *J. Comput. Chem.* **2009**, *30*, 1545.
22. Momany, F. A.; Rone, R. *J. Comput. Chem.* **1992**, *13*, 888.
23. Baell, J. B.; Holloway, G. A. *J. Med. Chem.* **2010**, *53*, 2719.
24. Singh, R.; Masuda, E. S.; Payan, D. G. *J. Med. Chem.* **2012**, *55*, 3614.